# Galactic tide and orbital evolution of comets

**L. Kómar · J. Klačka · P. Pástor**

**Abstract** Equation of motion for a comet in the Oort cloud is numerically solved. Orbital evolution of the comet under the action of the gravity of the Sun and the Galaxy is presented for various initial conditions.

Oscillations of the Sun with respect to the galactic equatorial plane are taken into account. Real values of physical quantities concerning the gravitational action of the galactic neighbourhood of the Sun are important. The results are compared with currently used more simple models of the galactic tide. It turns out that physically improved models yield results which significantly differ from the results obtained on the basis of the conventional models. E.g., the number of returns of the comets into the inner part of the Solar System are about two times greater than it is in the conventional models.

It seems that a comet from the Oort cloud can be a source of the dinosaurs extinction at about 65 Myr ago. A close encounter of a star or an interstellar cloud disturbed a comet of the Oort cloud in the way that its semi-major axis increased/decreased above the value $5 \times 10^4$ AU and the comet hit the Earth.

**Keywords** Oort cloud · Galaxy · Comets · Equation of motion · Orbital evolution

## 1 Introduction

Global galactic gravitational field influences motion of a comet in the Öpik-Oort cloud (Öpik 1932, Oort 1950) in the form of the galactic tide. The motion of the comet with respect to the Sun is important in better understanding of the Oort cloud. This paper deals with detailed numerical solution of the equation of motion of the comet under the gravity of the Sun and the galactic tide. We consider equation of motion presented by Klačka (2009a, 2009b). The $x-$ and $y-$ components of the acceleration come not only from the $x-$ and $y-$ components of the position of the comet, but also from the $z-$component of the position due to the gravity of the galactic disk. Our paper provides detailed numerical solutions of the equation of motion. The importance of the $\Gamma$-terms is tested. Comparison with the conventional models of galactic tide is discussed (see,

Faculty of Mathematics, Physics and Informatics, Comenius University
Mlynská dolina, 842 48 Bratislava, Slovak Republic
E-mail: {komar,klacka,pavol.pastor}@fmph.uniba.sk

e.g., Mihalas 1968, Heilser and Tremaine 1986, Levison et al. 2001, Dybczynski et al. 2008).

## 2 Orbital elements

We discuss several models of galactic tide. Each of them is represented by an equation of motion. The equation of motion is numerically solved. On the basis of the positional and velocity vectors at each position, we can find orbital elements and their evolution. We can use Eq. (47) in Klačka (2004) for this purpose (the right-hand side of the last equation in Eq. 47 contains $1/e$ instead of 1). We can summarize the equations in the following form [osculating orbital elements: $a$ – semi-major axis; $e$ – eccentricity; $i$ – inclination of the orbital plane to the reference plane – galactic equatorial plane; $\Omega$ – longitude of the ascending node; $\omega$ – longitude of pericenter (the argument of pericenter/perihelion); $q$ – perihelion distance; $Q$ – aphelion distance; $\Theta$ is the position angle of the particle on the orbit, when measured from the ascending node in the direction of the particle's motion, $\Theta = \omega + f$]:

$$
\begin{aligned}
\mathbf{r} &= (\xi, \eta, \zeta) \ , \quad r = |\mathbf{r}| \ , \\
\mathbf{v} &\equiv \dot{\mathbf{r}} = (\dot{\xi}, \dot{\eta}, \dot{\zeta}) \ , \\
E &= \frac{1}{2} \ \mathbf{v}^2 \ - \ \frac{G \ M_\odot}{r} \ , \\
\mathbf{H} &= \mathbf{r} \times \mathbf{v} \ , \\
p &= \frac{\mathbf{H}^2}{G \ M_\odot} \ , \\
e &= \sqrt{1 \ + \ 2 \ \frac{p \ E}{G \ M_\odot}} \ , \\
a &= \frac{p}{1 - e^2} \ , \\
E &= - \ \frac{G \ M_\odot}{2 \ p} \ \left(1 - e^2\right) \ , \\
q &= a(1 - e) \ , \\
Q &= a(1 + e) \ , \\
i &= \arccos \left( \frac{H_z}{|\mathbf{H}|} \right) \ , \\
\sin \Omega &= \frac{H_\xi}{\sqrt{H_\xi^2 + H_\eta^2}} \ , \\
\cos \Omega &= - \ \frac{H_\eta}{\sqrt{H_\xi^2 + H_\eta^2}} \ , \\
\sin \omega &= \frac{|\mathbf{H}|}{\sqrt{H_\xi^2 + H_\eta^2}} \ \frac{1}{r \ e} \ \times \ S1 \\
S1 &= - \ \frac{\eta \ H_\xi \ - \ \xi \ H_\eta}{|\mathbf{H}|} \ \frac{\mathbf{v} \cdot \mathbf{e}_R}{\sqrt{G \ M_\odot / p}} \ + \ \zeta \ \left( \frac{\mathbf{v} \cdot \mathbf{e}_T}{\sqrt{G \ M_\odot / p}} \ - \ 1 \right) \ ,
\end{aligned}
$$

$$\cos\omega = \frac{|\mathbf{H}|}{\sqrt{H_\xi^2 + H_\eta^2}} \, \frac{1}{r \; e} \; \times \; C1$$

$$C1 = \frac{\eta \; H_\xi \; - \; \xi \; H_\eta}{|\mathbf{H}|} \; \left( \frac{\mathbf{v} \cdot \mathbf{e}_T}{\sqrt{G \; M_\odot / p}} \; - \; 1 \right) \; + \; \zeta \; \frac{\mathbf{v} \cdot \mathbf{e}_R}{\sqrt{G \; M_\odot / p}} \; ,$$

$$\mathbf{e}_R = \frac{\mathbf{r}}{r} \; ,$$

$$\mathbf{e}_N = \frac{\mathbf{H}}{|\mathbf{H}|} \; ,$$

$$\mathbf{e}_T = \mathbf{e}_N \times \mathbf{e}_R \; . \tag{1}$$

## 3 Current models

### 3.1 Simple model

The most simple model considering galactic tide is described by the well-known equation of motion (see, e. g., Mihalas 1968, Heisler and Tremaine 1986)

$$\frac{d^2\xi}{dt^2} = - \; \frac{GM_\odot}{r^3} \; \xi$$

$$\frac{d^2\eta}{dt^2} = - \; \frac{GM_\odot}{r^3} \; \eta$$

$$\frac{d^2\zeta}{dt^2} = - \; \frac{GM_\odot}{r^3} \; \zeta \; - \; \left[ 4 \; \pi \; G \; \varrho \; + \; 2 \left( A^2 \; - \; B^2 \right) \right] \; \zeta$$

$$r = \sqrt{\xi^2 \; + \; \eta^2 \; + \; \zeta^2} \; , \tag{2}$$

where $G$ is the gravitational constant, $M_\odot$ is mass of the Sun, $\rho$ is the mass density of the Galaxy and $A$, $B$ are Oort constants. Numerical solution of the equation of motion was presented by Pretka and Dybczynski (1994) and secular evolution by Klačka and Gajdošík (2001):

$$\left\langle \frac{da}{dt} \right\rangle = 0$$

$$\left\langle \frac{de}{dt} \right\rangle = \frac{5}{4} \; k \; \sqrt{\frac{a^3}{\mu}} \; (\sin \; i)^2 \; [\sin(2\omega)] \; e \; \sqrt{1 \; - \; e^2}$$

$$\left\langle \frac{di}{dt} \right\rangle = \frac{1}{2} [\sin(2\omega)] (\sin \; i) \; \frac{(1 - e_0^2) \; (\cos \; i_0)^2 \; - \; (\cos \; i)^2}{\sqrt{1 \; - \; e_0^2} \; \cos \; i_0}$$

$$\left\langle \frac{d\omega}{dt} \right\rangle = \frac{[1/5 \; - \; (\sin \; \omega)^2](1 \; - \; e_0^2)(\cos \; i_0)^2 \; + \; (\sin \; \omega)^2 (\cos \; i)^4}{\sqrt{1 \; - \; e_0^2} \; (\cos \; i_0)(\cos \; i)} \; ,$$

$$k = 4 \; \pi \; G \; \varrho \; + \; 2 \left( A^2 \; - \; B^2 \right) \; . \tag{3}$$

### 3.2 Standard model

Previous section presented the most simple action of galactic tide. A more elaborated model is often used (Heisler and Tremaine 1986, Levison et al. 2001, Dybczynski et al.

2008):

$$\begin{aligned}
\frac{d^2\xi}{dt^2} &= -\frac{GM_\odot}{r^3}\,\xi + (A-B)\left[A+B+2A\cos\left(2\,\omega_0 t\right)\right]\,\xi \\
&\quad - 2A(A-B)\sin\left(2\,\omega_0 t\right)\,\eta \\
\frac{d^2\eta}{dt^2} &= -\frac{GM_\odot}{r^3}\,\eta - 2A(A-B)\sin\left(2\,\omega_0 t\right)\,\xi \\
&\quad + (A-B)\left[A+B-2A\cos\left(2\,\omega_0 t\right)\right]\,\eta \\
\frac{d^2\zeta}{dt^2} &= -\frac{GM_\odot}{r^3}\,\zeta - \left[4\,\pi\,G\,\varrho + 2\left(A^2 - B^2\right)\right]\,\zeta \\
r &= \sqrt{\xi^2 + \eta^2 + \zeta^2}\,, \\
\omega_0 &= A - B\,,
\end{aligned} \tag{4}$$

where $G$ is the gravitational constant, $M_\odot$ is the mass of the Sun and the numerical values of the other relevant quantities are

$$\begin{aligned}
A &= 13.0 \text{ km s}^{-1} \text{ kpc}^{-1}\,, \\
B &= -\,13.0 \text{ km s}^{-1} \text{ kpc}^{-1}\,, \\
\varrho &= 0.10 \text{ M}_\odot \text{ pc}^{-3}\,.
\end{aligned} \tag{5}$$

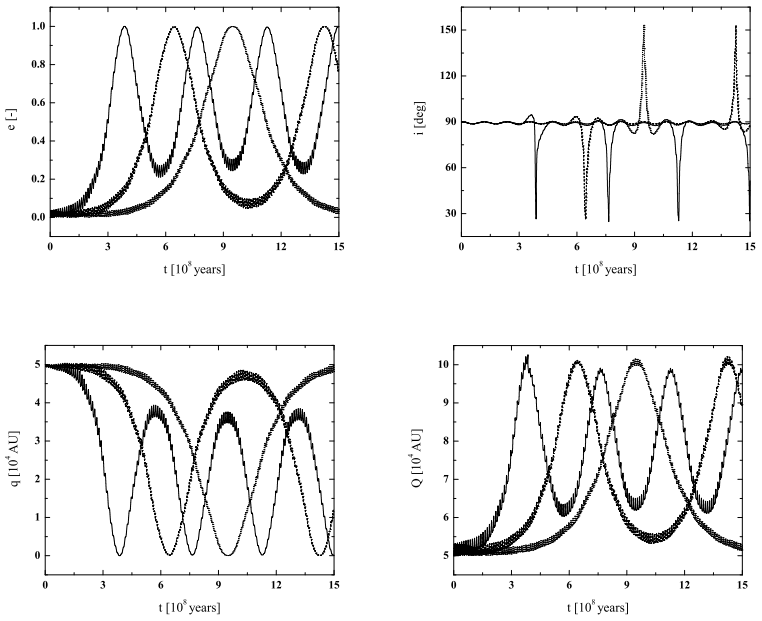


**Fig. 1** Orbital evolution of the comet situated in the Oort cloud with $a_{in} = 5 \times 10^4$ AU, $e_{in} \approx 0$, $i_{in} = 90°$ under the influence of the solar gravity and the galactic tide based on the standard model for various mass densities in the neighbourhood of the Sun: $\rho = 0.075$ $\text{M}_\odot$ $\text{pc}^{-3}$ (dotted line), $\rho = 0.1$ $\text{M}_\odot$ $\text{pc}^{-3}$ (dashed line), $\rho = 0.15$ $\text{M}_\odot$ $\text{pc}^{-3}$ (solid line).

Fig. 1 represents the numerical solution of Eqs. (4) and (5). It shows the orbital evolution of the comet situated in the Oort cloud of comets ($a_{in} = 5 \times 10^4$ AU) with initial almost circular orbit perpendicular to the plane of the galactic equator ($e_{in} \approx 0$, $i_{in} = 90°$). Solar gravity and the galactic tide in terms of the standard model are considered for various local densities $\rho$ in the neighbourhood of the Sun.

In the literature the values of the local density span from $\rho = 0.075$ $M_\odot$ $pc^{-3}$ (Crézé et al. 1998) to $\rho = 0.185$ $M_\odot$ $pc^{-3}$ (Bahcall 1984). As it is shown in Fig. 1, the orbital evolution of the comet initially situated in the Oort cloud is very sensitive to the local density. For comparison we used the values $\rho = 0.075$ $M_\odot$ $pc^{-3}$, $\rho = 0.1$ $M_\odot$ $pc^{-3}$ (Levison et al. 2001) and $\rho = 0.15$ $M_\odot$ $pc^{-3}$ (Wiegert and Tremaine 1999).

### 3.3 Comparison of the current models

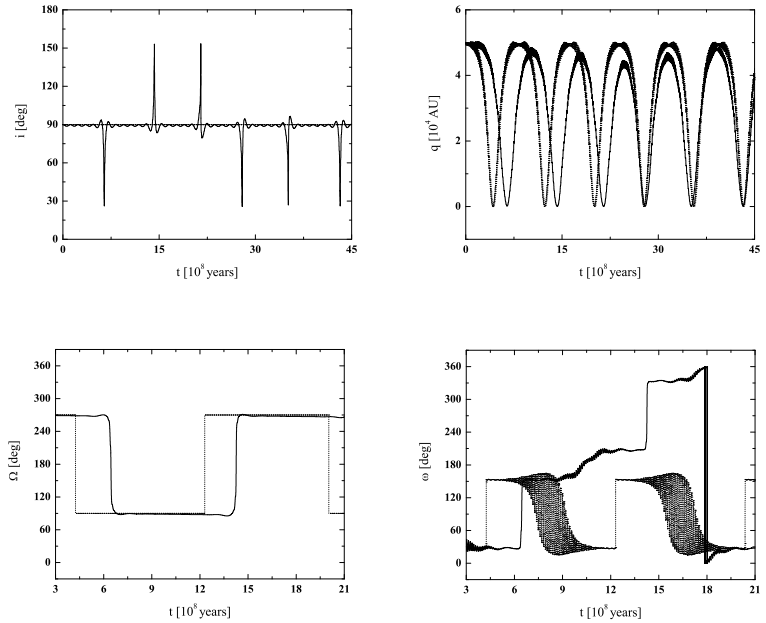


**Fig. 2** Orbital evolution of the comet situated in the Oort cloud with $a_{in} = 5 \times 10^4$ AU, $e_{in} \approx 0$, $i_{in} = 90°$ under the influence of the solar gravity and the galactic tide for the simple (dotted line) and the standard (solid line) models. Local density $\rho = 0.1$ $M_\odot$ $pc^{-3}$ is considered for both models.

Figs. 2 and 3 compare orbital evolution of the comet calculated from the models discussed above.

Fig. 2 shows the difference between the simple and the standard model for the the comet with initial values $a_{in} = 5 \times 10^4$ AU, $e_{in} \approx 0$ and $i_{in} = 90°$. For the standard model (solid line) the number of returns of the comet to the inner part of the Solar System (perihelion distance less than 150 AU, approximately) is 5, while for the simple

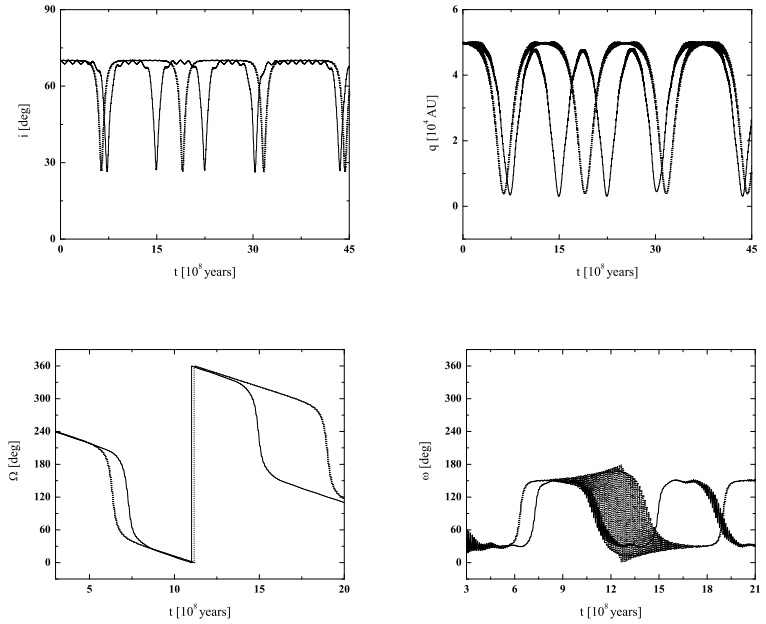


**Fig. 3** Orbital evolution of the comet situated in the Oort cloud with $a_{in} = 5 \times 10^4$ AU, $e_{in} \approx 0$, $i_{in} = 70^\circ$ under the influence of the solar gravity and the galactic tide for the simple (dotted line) and the standard (solid line) models. Local density $\rho = 0.1$ $M_\odot$ pc$^{-3}$ is considered for both models.

model (dotted line) the number of returns is only 4 during the integration time $4.5 \times 10^9$ years. The difference between the two current models are also shown in the evolution of the inclination $i$, longitude of the ascending node $\Omega$ and longitude of pericenter $\omega$ in Fig. 2.

Fig. 3 represents the case when the initial inclination of the comet is $i_{in} = 70^\circ$. Again, semi-major axis and eccentricity are $a_{in} = 5 \times 10^4$ AU, $e_{in} \approx 0$. In this special case $< di/dt > = 0$ for the simple model (see Eq. 3). For the standard model the orbit of the comet can be prograde, but also retrograde. The orbit of the comet is always prograde for $i_{in} < 90^\circ$. The orbit of the comet is always retrograde for $i_{in} > 90^\circ$.

The number of returns of the comet to the inner part of the Solar System is 6, if $i_{in} = 90^\circ$, both for the simple and standard models.

For the difference between the number of cometary returns for the current models and more physical models compare Figs. 2, 3 with Figs. 5-8.

## 4 Improved models

Current models discussed in Sec. 3 must be treated as a rough approximation to reality. At present, an improved and more realistic physical access to galactic tide is in disposal (Klačka 2009a, 2009b). This section presents orbital evolution for the improved access to galactic tide. The results are compared to the evolution for the standard model.

4.1 Model I

We are interested in the motion of the comet with respect to the Sun. The Sun is moving in a distance $R_0 = 8$ kpc from the center of the Galaxy. Currently, the Sun is situated 30 pc above the galactic equatorial plane ($Z_0 = 30$ pc). Besides rotational motion with the speed $(A - B)\ R_0$ the Sun moves with the speed 7.3 km/s in the direction normal to the galactic plane. Positional vector of the comet with respect to the Sun is $\mathbf{r} = (\xi, \eta, \zeta)$.

Equation of motion is taken in the form (Klačka 2009, Eq. 29)

$$\begin{aligned}
\frac{d^2\xi}{dt^2} &= -\frac{GM_\odot}{r^3}\,\xi + (A-B)\left[A+B+2A\cos\left(2\,\omega_0 t\right)\right]\,\xi \\
&\quad - 2A(A-B)\sin\left(2\,\omega_0 t\right)\,\eta \\
&\quad + (A-B)^2\left(\Gamma_1/(b^2+Z_0^2)^{1/2}+\Gamma_2\right)\,R_0\,Z_0\,\cos\left(\omega_0 t\right)\,\zeta\ , \\
\frac{d^2\eta}{dt^2} &= -\frac{GM_\odot}{r^3}\,\eta - 2A(A-B)\sin\left(2\,\omega_0 t\right)\,\xi \\
&\quad + (A-B)\left[A+B-2A\cos\left(2\,\omega_0 t\right)\right]\,\eta \\
&\quad - (A-B)^2\left(\Gamma_1/(b^2+Z_0^2)^{1/2}+\Gamma_2\right)\,R_0\,Z_0\,\sin\left(\omega_0 t\right)\,\zeta\ , \\
\frac{d^2\zeta}{dt^2} &= -\frac{GM_\odot}{r^3}\,\zeta - \left[4\,\pi\,G\,\varrho + 2\left(A^2 - B^2\right)\right]\,\zeta \\
&\quad - 4\,\pi\,G\,\varrho'\,Z_0\left[\cos\left(\omega_0 t\right)\,\xi - \sin\left(\omega_0 t\right)\,\eta\right]\ , \\
\frac{d^2 Z_0}{dt^2} &= -\left[4\,\pi\,G\,\varrho + 2\left(A^2 - B^2\right)\right]\,Z_0\ , \\
r &= \sqrt{\xi^2+\eta^2+\zeta^2}\ , \\
\omega_0 &= A - B\ ,
\end{aligned} \tag{6}$$

where $G$ is the gravitational constant, $M_\odot$ is the mass of the Sun and the numerical values of the other relevant quantities are

$$\begin{aligned}
A &= 14.25\ \mathrm{km\ s^{-1}\ kpc^{-1}}\ , \\
B &= -\,13.89\ \mathrm{km\ s^{-1}\ kpc^{-1}}\ , \\
\Gamma_1 &= 0.084\ \mathrm{kpc^{-1}}\ , \\
\Gamma_2 &= 0.008\ \mathrm{kpc^{-2}}\ , \\
\varrho &= 0.143\ \mathrm{M_\odot\ pc^{-3}}\ , \\
\varrho' &= -\,0.0425\ \mathrm{M_\odot\ pc^{-3}\ kpc^{-1}}\ , \\
b &= 0.25\ \mathrm{kpc}\ .
\end{aligned} \tag{7}$$

Eqs. (6) - (7) correspond to the model of the Galaxy presented by Dauphole et al. (1996).

Fig. 4 shows the position of the Sun with respect to the plane of the galactic equator as a function of time for two improved models. The period of oscillations of the Sun with respect to the plane of galactic equator is $6.96 \times 10^7$ years for the Model I and $7.26 \times 10^7$ years for the Model II. Maximal distance of the Sun is 87.8 pc from the plane of the galactic equator for the Model I and 91.14 pc for the Model II.

The Sun is always located in the plane of galactic equator for the current models discussed in Sec. 3.

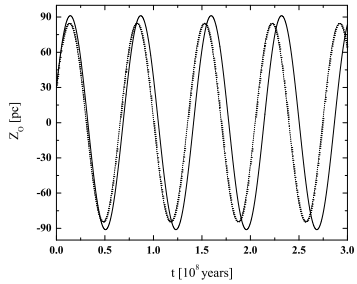


**Fig. 4** Position of the Sun with respect to the plane of the galactic equator as a function of time. Galactic tides for the Model I (dotted line) and the Model II (solid line) are considered.

Figs. 5 and 6 depict the orbital evolution of the comet as a numerical solution of Eq. (6), if also Eqs. (1) and (7) are taken into account. Comet is initially situated on the almost circular orbit ($e_{in} \approx 0$) in the Oort cloud, $a_{in} = 5 \times 10^4$ AU. Orbital evolutions for two different initial inclinations are presented, $i_{in} = 90^\circ$ in Fig. 5 and $i_{in} = 70^\circ$ in Fig. 6. For comparison, the initial conditions of the comet are the same as for numerical calculations presented in Sec. 3.

Figs. 5 and 6 represent the evolution of eccentricity $e$, inclination $i$, , longitude of the ascending node $\Omega$, longitude of pericenter $\omega$, perihelion distance $q$ and aphelion distance $Q$ during $4.5 \times 10^9$ years. Semimajor axes are practically constant during the whole integration time for both presented inclinations.

Evolutions of the orbital elements in Figs. 5, 6 show the main differences between the current models described in Sec 3 and our improved Model I (compare with Figs. 2, 3 ).

| | Standard model | | Model I | |
|---|---|---|---|---|
| $i_{in}$ | $< q >$ [AU] | $< Q >$ [AU] | $< q >$ [AU] | $< Q >$ [AU] |
| 70° | 33792 | 66889 | 29484 | 71526 |
| 90° | 29827 | 70685 | 27574 | 73605 |
| 120° | 36614 | 63922 | 32934 | 67884 |

**Table 1** Mean values of the perihelion and aphelion distances during the integration time $4.5 \times 10^9$ years for the standard model and the Model I. Results for three different initial inclinations of the comet with $a_{in} = 5 \times 10^4$ AU, $e_{in} \approx 0$ are presented.

Table 1 presents mean values of the perihelion and aphelion distances for the standard model and the Model I. Various initial inclinations are presented. Both the standard model and the Model I have minima of the mean values of the perihelion distances for the initial inclination $i_{in} = 90^\circ$. Also the maxima of the mean values of the aphelion distances belong to the initial inclination $i_{in} = 90^\circ$. On the basis of our calculations we can state that the Model I shows lower mean values of the perihelion distances than the standard model and this holds irrespective to initial inclinations. The Model I also shows higher mean values of the aphelion distances than the standard model, again irrespective of the initial inclinations.

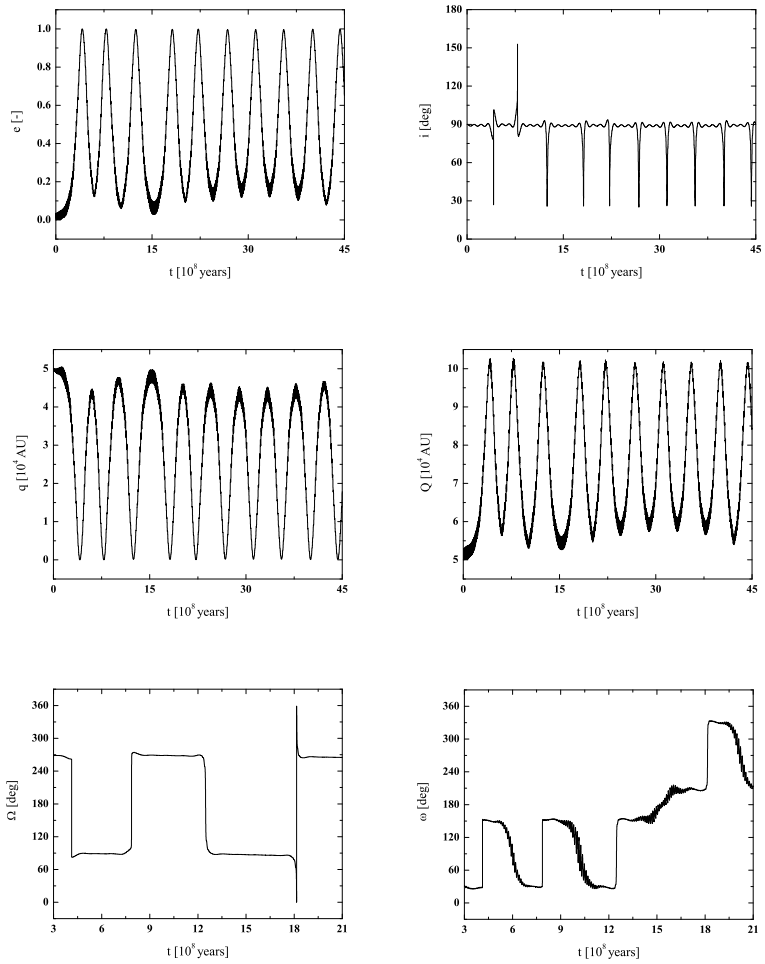


**Fig. 5** Orbital evolution of the comet situated in the Oort cloud with $a_{in} = 5 \times 10^4$ AU, $e_{in} \approx 0$, $i_{in} = 90°$ under the influence of the solar gravity and the galactic tide for the Model I.

### 4.2 Model II

Equation of motion is taken in the form (Klačka 2009a, Eqs. 26-27):

$$\begin{aligned}
\frac{d^2\xi}{dt^2} = & - \frac{GM_\odot}{r^3}\ \xi\ +\ (A-B)\left[A+B+2A\cos\left(2\ \omega_0 t\right)\right]\ \xi \\
& - 2A(A-B)\sin\left(2\ \omega_0 t\right)\ \eta \\
& + 2(A-B)^2\left(\Gamma_1 - \Gamma_2 Z_0^2\right)\ R_0\ Z_0\ \cos\left(\omega_0 t\right)\ \zeta\ , \\
\frac{d^2\eta}{dt^2} = & - \frac{GM_\odot}{r^3}\ \eta\ -\ 2A(A-B)\sin\left(2\ \omega_0 t\right)\ \xi \\
& + (A-B)\left[A+B-2A\cos\left(2\ \omega_0 t\right)\right]\ \eta
\end{aligned}$$

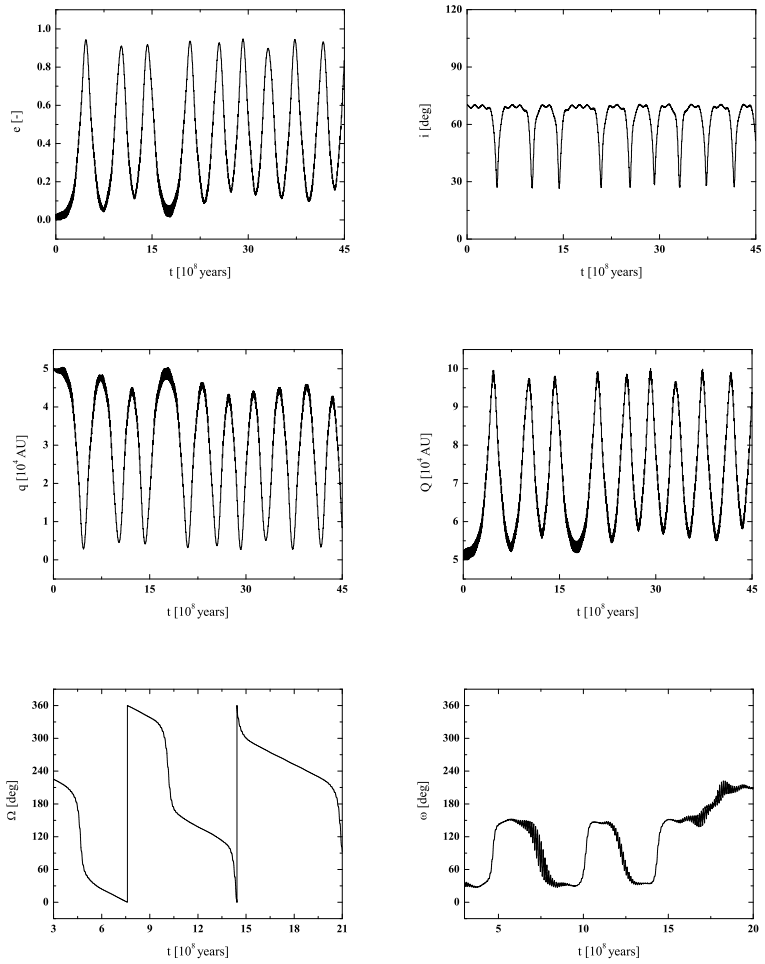


**Fig. 6** Orbital evolution of the comet situated in the Oort cloud with $a_{in} = 5 \times 10^4$ AU, $e_{in} \approx 0$, $i_{in} = 70^\circ$ under the influence of the solar gravity and the galactic tide for the Model I.

$$
\begin{aligned}
&- 2(A-B)^2 \left(\Gamma_1 - \Gamma_2 Z_0^2\right)\ R_0\ Z_0\ \ \sin(\omega_0 t)\ \zeta\ , \\
\frac{d^2\zeta}{dt^2} &= -\frac{GM_\odot}{r^3}\ \zeta\ -\ \left[4\ \pi\ G\ \varrho\ +\ 2\left(A^2\ -\ B^2\right)\right]\ \zeta \\
&- 4\ \pi\ G\ \varrho'\ Z_0\left[\cos(\omega_0 t)\ \xi\ -\ \sin(\omega_0 t)\ \eta\right]\ , \\
\frac{d^2 Z_0}{dt^2} &= -\ \left[4\ \pi\ G\ \varrho\ +\ 2\left(A^2\ -\ B^2\right)\right]\ Z_0\ , \\
r &= \sqrt{\xi^2\ +\ \eta^2\ +\ \zeta^2}\ , \\
\omega_0 &= A\ -\ B\ ,
\end{aligned}
\tag{8}
$$

where $G$ is the gravitational constant, $M_\odot$ is the mass of the Sun and the numerical values of the other relevant quantities are

$$\begin{aligned} A &= 14.2 \text{ km s}^{-1} \text{ kpc}^{-1} , \\ B &= -\ 12.4 \text{ km s}^{-1} \text{ kpc}^{-1} , \\ \Gamma_1 &= 0.124 \text{ kpc}^{-2} , \\ \Gamma_2 &= 1.586 \text{ kpc}^{-4} , \\ \varrho &= 0.130 \text{ M}_\odot \text{ pc}^{-3} , \\ \varrho' &= -\ 0.037 \text{ M}_\odot \text{ pc}^{-3} \text{ kpc}^{-1} , \end{aligned} \tag{9}$$

see Eqs. (20)-(21) in Klačka (2009). If one wants to use other values of the Oort constants $A$ and $B$, then he can use the following equation for calculation of mass density in the neighborhood of the Sun:

$$\begin{aligned} \varrho &= \varrho_{disk} \ + \ \varrho_{halo} , \\ \varrho_{disk} &= 0.126 \text{ M}_\odot \text{ pc}^{-3} , \\ \varrho_{halo} &= (4\pi G)^{-1}[X(Galaxy) - X(disk) - X(bulge)] , \\ X(Galaxy) &\equiv -(A-B) \times (A+3B) \\ X(disk) &= 396.898 \text{ km}^2 \text{ s}^{-2} \text{ kpc}^{-2} , \\ X(bulge) &= 0.625 \text{ km}^2 \text{ s}^{-2} \text{ kpc}^{-2} . \end{aligned} \tag{10}$$

The value $X(Galaxy) = 611.800 \text{ km}^2 \text{ s}^{-2} \text{ kpc}^{-2}$ holds for $A = 14.2 \text{ km s}^{-1} \text{ kpc}^{-1}$ and $B = -\ 12.4 \text{ km s}^{-1} \text{ kpc}^{-1}$. Moreover, Eq. (17) of Klačka (2009) can be used.

Figs. 7 and 8 represent the orbital evolution of a comet as a numerical solution of Eq. (8), if also Eqs. (1) and (9) are taken into account. The comet is initially situated in the Oort cloud ( $a_{in} = 5 \times 10^4$ AU) on the initially almost circular orbit as well as in pervious cases. Orbital evolutions for two different initial inclinations are presented, $i_{in} = 90^\circ$ in Fig. 7, $i_{in} = 70^\circ$ in Fig. 8.

Figs. 7 and 8 depict the evolution of eccentricity $e$, inclination $i$, , longitude of the ascending node $\Omega$, longitude of pericenter $\omega$, perihelion distance $q$ and aphelion distance $Q$ during the current lifetime of the Solar System. Semimajor axes are practically constant during the whole integration time for both presented inclinations.

The evolutions of the orbital elements in Figs. 7 and 8 show the main differences between the current models described in Sec. 3 and our improved physical Model II (compare with Figs. 2 and 3 ).

| | Standard model | | Model II | |
|---|---|---|---|---|
| $i_{in}$ | $< q >$ [AU] | $< Q >$ [AU] | $< q >$ [AU] | $< Q >$ [AU] |
| 70° | 33792 | 66889 | 25157 | 75766 |
| 90° | 29827 | 70685 | 27306 | 73757 |
| 120° | 36614 | 63922 | 33768 | 66971 |

**Table 2** Mean values of the perihelion and aphelion distances during the integration time $4.5 \times 10^9$ years for the standard model and the Model II. Three different initial inclinations of the comet with $a_{in} = 5 \times 10^4$ AU, $e_{in} \approx 0$ are considered.

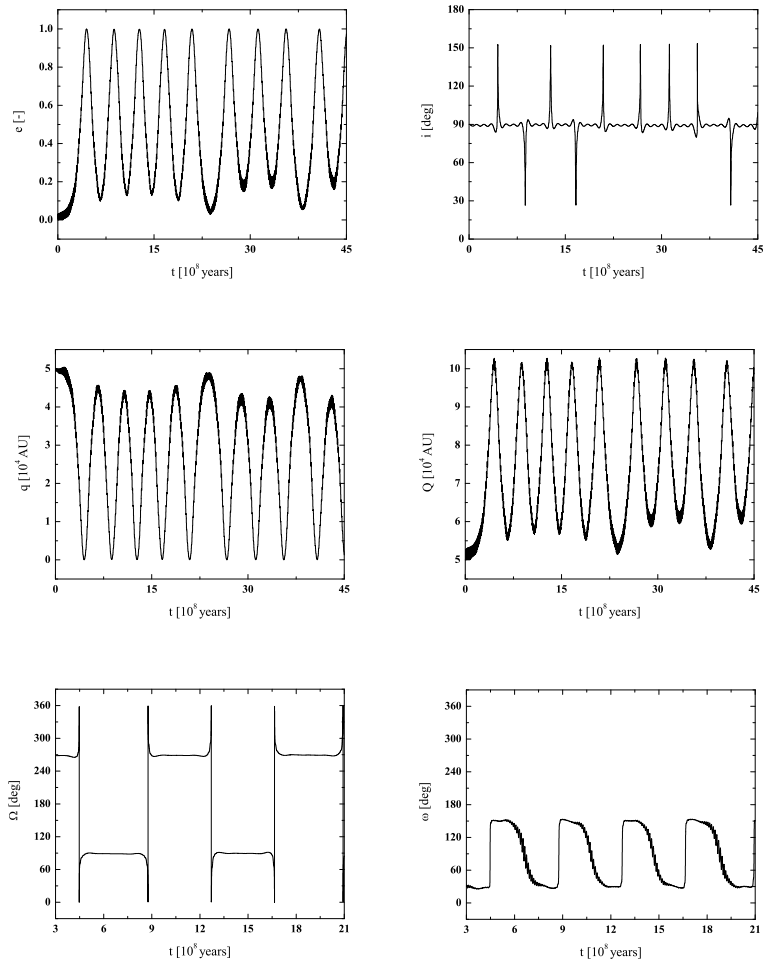


**Fig. 7** Orbital evolution of the comet with initial values $a_{in} = 5 \times 10^4$ AU, $e_{in} \approx 0$, $i_{in} = 90^\circ$ under the influence of the solar gravity and the galactic tide for the Model II

Table 2 contains mean values of the perihelion and aphelion distances for the standard model and the Model II. Various initial inclinations are presented as well as in Table 1. For the standard model, the minimum of the mean value of the perihelion distance belongs to the initial inclination $i_{in} = 90^\circ$, but for the Model II the least value belongs to $i_{in} = 70^\circ$. Maximum of the mean value of the aphelion distance belongs to the initial inclination $i_{in} = 90^\circ$ for the standard model and to $i_{in} = 70^\circ$ for the Model II. The Model II shows lower mean values of the perihelion distances than the standard model for all of the presented initial inclinations. The Model II also shows higher mean values of the aphelion distances than the standard model for all of the presented initial inclinations.

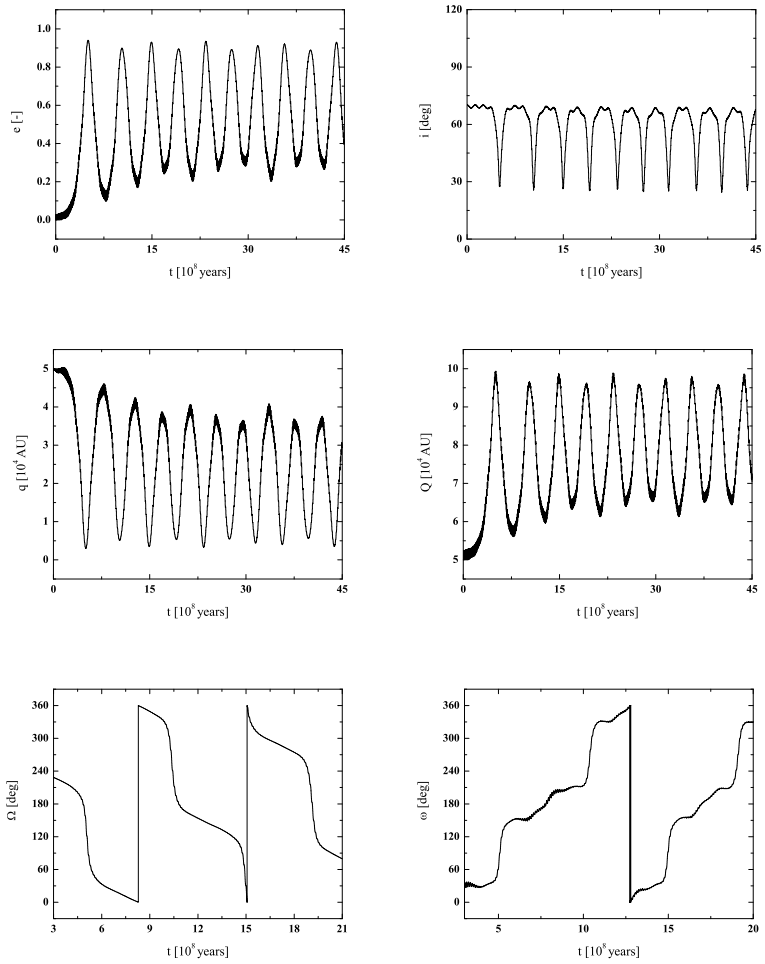


**Fig. 8** Orbital evolution of the comet with $a_{in} = 5 \times 10^4$ AU, $e_{in} \approx 0$, $i_{in} = 70°$ under the influence of the solar gravity and the galactic tide for the Model II.

## 5 Discussion

Models I and II are based on more realistic physics than the standard or simple models. The Model I corresponds to the model of the Galaxy by Dauphole et al. (1986). This model of the Galaxy does not respect several important observational facts. It does not yield a flat rotation curve for great galactocentric distances. Mass density in the vicinity of the Sun is relatively large in comparison to newer values. Moreover, it does not produce the observed values of the Oort constants. Both of these observational facts are taken into account in the model of the Galaxy which served for our Model II (Klačka 2009a). This is the reason why we consider the Model II to be more relevant

than the Model I. In any case, both of these models take into account motion of the Sun in a more realistic way than it is considered in the simple and standard models.

As a consequence of the previous discussion we can stress several facts. The standard model yields mean value of the perihelion distance in $\approx 35\%$ higher than the real value for $i_{in} = 70^\circ$. This follows from Tables 1 and 2: $< q >$ (standard model) / $< q >$ (Model I) = 1.146, $< q >$ (standard model) / $< q >$ (Model II) = 1.343. Moreover, the Model II is the only of the discussed models which yields $\langle q \rangle (i_{in} = 70^\circ) < \langle q \rangle (i_{in} = 90^\circ)$.

Let $\tau_q$ is a timescale on which a comet's perihelion changes in $\Delta q$. Let us consider Fig. 7 and Table 3 for finding $\tau_q$ for $t \approx 2.3 \times 10^9$ years. The case of maximum in $q = q(t)$ yields:
$\tau_q$ ($q = 4.8 \times 10^4$ AU, $\Delta q = 0.4 \times 10^4$ AU; reality) $= 9.4 \times 10^7$ yrs,
while the relation presented by Levison and Dones (2007, p. 583) yields
$\tau_q$ ($q = 4.8 \times 10^4$ AU, $\Delta q = 0.4 \times 10^4$ AU; literature) $= 4.8 \times 10^6$ yrs.
The mathematical relation yields 20-times smaller value than the real value. Now, let us consider minimum in $q = q(t)$ for $t \approx 2.3 \times 10^9$ years. The real value is
$\tau_q$ ($q = 1/4 \times 10^4$ AU, $\Delta q = 1/2 \times 10^4$ AU; reality) $= 4.7 \times 10^7$ yrs,
while the mathematical relation yields
$\tau_q$ ($q = 1/4 \times 10^4$ AU, $\Delta q = 1/2 \times 10^4$ AU; literature) $= 2.6 \times 10^7$ yrs,
or, using the value $q = 38$ AU from Table 3,
$\tau_q$ ($q = 38$ AU, $\Delta q = 1/2 \times 10^4$ AU; literature) $= 2.1 \times 10^8$ yrs.
Of course, smaller value of $\Delta q$ may be taken into account. We can say that
$0.5 < \tau_q$ (literature) / $\tau_q$ (reality) $< 20$.

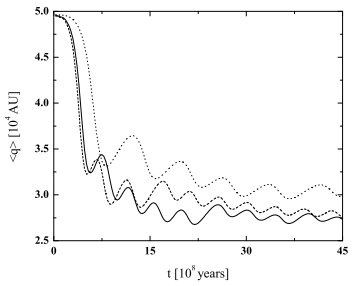


**Fig. 9** Comparison of the evolution of the mean perihelion distance of the comet with $a_{in} = 5 \times 10^4$ AU, $e_{in} \approx 0$, $i_{in} = 90^\circ$ for the standard model (dotted line), the Model I (dashed line) and the Model II (solid line).

Table 3 presents minimal values of perihelion distances for the calculated models. While the standard model yields three cases with $q_{min} < 50$ AU, the Model I shows that the same situation occurs in one case, only. As we have discussed above, the relevant Model II yields six cases with $q_{min} < 50$ AU. Table 4 presents values of the same quantities for initial galactocentric inclination 70 degrees. As a result we can state that the smallest values of $q_{min}$ exist for initial inclination corresponding to 90 degrees. Fig. 9 depicts time average of evolution of perihelion distance $\langle q \rangle \equiv \langle q(t) \rangle =$

| Standard model | | Model I | | Model II | |
|---|---|---|---|---|---|
| q [AU] | Q [AU] | q [AU] | Q [AU] | q [AU] | Q [AU] |
| 113.0 | 101142.6 | 1.5 | 102594.9 | 24.7 | 102713.9 |
| 38.7 | 102137.5 | 143.8 | 102692.2 | 101.3 | 101620.5 |
| 3.7 | 101971.8 | 115.7 | 101718.5 | 93.4 | 102701.1 |
| 71.9 | 101056.8 | 50.5 | 102034.1 | 104.2 | 101700.1 |
| 21.2 | 101258.6 | 187.5 | 102263.4 | 38.1 | 102769.8 |
| 111.6 | 100130.6 | 194.9 | 101536.0 | 25.9 | 102648.5 |
| – | – | 192.1 | 101758.7 | 43.7 | 102744.2 |
| – | – | 90.5 | 101707.7 | 1.0 | 102455.4 |
| – | – | 149.0 | 102142.4 | 37.5 | 102046.6 |
| – | – | – | 101552.9 | – | – |

**Table 3** Extremal perihelion and aphelion distances of the comet with $a_{in} = 5 \times 10^4$ AU, $e_{in} \approx 0$, $i_{in} = 90°$ during the integration time $4.5 \times 10^9$ years for the standard model, the Model I and the Model II.

| Standard model | | Model I | | Model II | |
|---|---|---|---|---|---|
| q [AU] | Q [AU] | q [AU] | Q [AU] | q [AU] | Q [AU] |
| 3465.38 | 98209.0 | 2883.6 | 99568.6 | 2968.3 | 99308.4 |
| 3036.7 | 98793.8 | 4539.5 | 97433.9 | 5067.2 | 96652.2 |
| 3063.5 | 98775.0 | 4168.9 | 98050.3 | 3446.5 | 98680.8 |
| 4466.9 | 96966.1 | 3190.1 | 99294.7 | 5299.0 | 96224.7 |
| 3062.8 | 98648.0 | 3689.2 | 98594.1 | 3267.2 | 98839.0 |
| – | – | 2714.9 | 100020.7 | 5441.0 | 95944.8 |
| – | – | 5114.2 | 96658.8 | 4385.5 | 97489.7 |
| – | – | 2753.9 | 99851.9 | 3970.5 | 97988.4 |
| – | – | 3407.8 | 99033.9 | 5573.5 | 95894.2 |

**Table 4** Extremal perihelion and aphelion distances of the comet with $a_{in} = 5 \times 10^4$ AU, $e_{in} \approx 0$, $i_{in} = 70°$ during the integration time $4.5 \times 10^9$ years for the standard model, the Model I and the Model II.

$\int_0^t q(t')dt'$ / $t$. The evolution of perihelion distance yields minimal values for the best physical model represented by our Model II.

The effect of Solar System's vertical motion above and below the galactic plane on the possible terrestrial mass extinctions was discussed in the past (see, e.g., Weissman 1990, Rampino and Stothers 1984, Schwartz and James 1984). Results corresponding to Fig. 4 show that period of the Solar System's vertical oscillations is $72.6 \times 10^6$ years. The last Sun's position in the galactic equatorial plane occured before $3.87 \times 10^6$ years. The last extinctions had to occur before $(3.87 \times 10^6 - \varepsilon \times a^{3/2})$ years, where semi-major axis $a$ of the comet is given in astronomical units and $0 < \varepsilon < 1$. The value of $\varepsilon$ describes the initial position of the comet on its orbit ($\varepsilon = 1/2$ corresponds to aphelion). Since the Solar System's oscilations are periodic, other possibilities are [(n $\times$ 72.6 / 2 + 3.87 ) $\times$ $10^6$ $-$ $\varepsilon$ $\times$ $a^{3/2}$ ] years, where $n$ is an integer number, which multiplies the half period of the Solar System's oscilations. Thus, also $(40.2 \times 10^6 - \varepsilon \times a^{3/2})$ years ($n = 1$), or, $(76.5 \times 10^6 - \varepsilon \times a^{3/2})$ years ($n = 2$) in the past. The values could correspond to the value of about $65 \times 10^6$ years of the late Cretaceous extinctions which included the disappearance of the dinosaurs (Rampino and Stothers 1984). The mass extictions on the Earth have periodic behaviour with the period approximately $33 \times 10^6$ years. The case $n = 2$ could occur for $a = 5.1 \times 10^4$ AU / $\varepsilon^{2/3}$. The comet was increasing its heliocentric distance for some part of its motion before the hit of the Earth, if $5.1 \times 10^4$ AU $< a < 8.1 \times 10^4$ AU. If the comet was still moving toward

the Sun, then $\varepsilon < 1/2$ and $a > 8.1 \times 10^4$ AU. The case $n = 1$, for $33 \times 10^6$ years in the past, yields $a = 3.73 \times 10^4$ AU / $\varepsilon^{3/2}$. If $\varepsilon < 1/2$, then $a > 5.9 \times 10^4$ AU. Similarly, the case $n = 3$, for $99 \times 10^6$ years in the past, yields $a = 5.74 \times 10^4$ AU / $\varepsilon^{3/2}$. Although the galactic tidal forces exclude stability of the Oort cloud for large values of semi-major axis, $a > 8 \times 10^4$ AU, a close encounter of a star or an interstellar cloud could disturb a comet of the Oort cloud. Finally, there is also a possibility that objects of interstellar origin hit the Earth.

There is an another feature of the effect of Solar System's vertical motion above and below the galactic plane on the possible terrestrial mass extinctions. We should await, on the basis of Fig. 7 and Table 3, that the period of possible exceptionally strong mass extinction is that the period of possible mass extinctions is (4.5-5.0) $\times 10^8$ years, if the galactic tide is the reason of the mass extinctions. This is twice the value presented by Schwartz and James (1984). It seems that we are not able to explain the major extinction events on the basis of the galactic tide alone.

## 6 Conclusion

The paper treats the effect of the galactic tide on a cometary motion with respect to the Sun. Our detailed numerical calculations show that the $\Gamma-$terms play an important role in cometary orbital evolution. The $\Gamma-$terms cause that periods of secular evolution of the orbital elements differ from the periods of conventional models. The real period is 1.7-times smaller than the period of the conventional models, if the initial cometary inclination is close to 90 degrees, eccentricity is close to zero and semi-major axis is about $5 \times 10^4$ AU. Shorter periods of secular evolution of orbital elements lead to the conclusion that frequency of cometary returns into the inner part of the Solar System is about two times higher than the frequency following from the conventional models.

A comet from the Oort cloud can be a source of the dinosaurs extinction at about 65 Myr ago. Either a close encounter of a star or an interstellar cloud disturbed a comet in the Oort cloud in the way that its semi-major axis increased/decreased above the value $5.1 \times 10^4$ AU and the comet hit the Earth. Or, an object of interstellar origin hit the Earth.

## Acknowledgement

This work was supported by the Scientific Grant Agency VEGA, Slovak Republic, grant No. 2/0016/09 and by the Comenius University grant UK/405/2009.

## References

1. Bahcall, J.N.: Self-consistent determinations of the total amount of matter near the Sun. Astrophys. J. 276, 169-181 (1984)
2. Crézé, M., Chereul, E., Bienayme, O., Pichon, C.: The distribution of nearby stars in phase space mapped by Hipparcos. Astron. Astrophys. 329, 920-936 (1998)
3. Dauphole, B., Colin, M., Odenkirchen, M., Tucholke, H.-J.: The mass distribution of the Milky Way deduced from globular cluster dynamics. In: Blitz, L. and Teuben, P. (eds.) Unsolved problems of the Milky Way, pp. 697-702. IAU Symposium 169 (1996)
4. Dybczynski, P.A., Leto, G., Jakubík, M., Paulech, T., Neslušan, L.: The simulation of the outer Oort cloud formation: The first giga-year of the evolution. Astron. Astrophys. 487, 345-355 (2008)

5. Heisler, J., Tremaine, S.: The influence of the galactic tidal field on the Oort comet cloud. Icarus 65, 13-26 (1986)
6. Klačka, J.: Electromagnetic radiation and motion of a particle. Celest. Mech. and Dynam. Astron. 89, 1-61 (2004)
7. Klačka, J.: Galactic tide. arXiv:astro-ph/0912.3112 (2009a)
8. Klačka, J.: Galactic tide in a noninertial frame of reference. arXiv:astro-ph/0912.3114 (2009b)
9. Klačka, J., Gajdošík, M.: Orbital motion in outer Solar System. In: Pretka-Ziomek, H., Wnuk, E., Seidelmann, P.K., Richardson, D. (eds.) Dynamics of Natural and Artificial Celestial Bodies, pp. 347-349. Kluwer Academic Press, Dordrecht, arXiv:astro-ph/9910041 (2001)
10. Levison, H., Dones, L., Duncan, M.J.: The origin of Halley-type comets: Probing the inner Oort cloud Astron. J. 121, 2253-2267 (2001)
11. Levison, H.F., Dones, L.: Comet Populations and Cometary Dynamics. In: McFadden, L.-A., Weismann, P.R., Johnson, T.V. (eds.) Encyclopedia of the Solar System, pp. 575-588. Elsevier (Academic Press), San Diego - London - Amsterdam - Burlington, second edition, chapter 31 (2007)
12. Mihalas, D., McRae Routly, P.: Galactic Astronomy. W.H. Freeman and Company, San Francisco, 257pp. (1968)
13. Oort, J.H.: The structure of the cloud of comets surrounding the Solar System and a hypothesis concerning its origin. Bull. Astron. Inst. Neth. 11, 91-110 (1950)
14. Öpik, E.J.: Note on Stellar Perturbations of Nearby Parabolic Orbits. Proceedings of the American Academy of Arts and Sciences 67, 169-182 (1932)
15. Pretka, H., Dybczynski, P.A.: The galactic disk influence on the Oort cloud cometary orbits. In: Kurzynska, K., Barlier, F., Seidelmann, P.K., Wytrzyszczak, I. (eds.) Dynamics and Astrometry of Natural and Artificial Celestial Bodies, pp. 299-304. Astronomical Observatory of A. Mickiewicz University, Poznan, Poland (1994)
16. Rampino, M.R., Stothers, R.B.: Terrestrial mass extinctions, cometary impacts and the Sun's motion perpandicular to the galactic plane. Nature 308, 709-712 (1984)
17. Schwartz, R.D., James, P.B.:. Periodic mass extinctions and the Sun's oscilation about the galactic plane. Nature 308, 712-713 (1984)
18. Weissman, P.R.: The Oort cloud. Nature 344, 825-830 (1990)
19. Wiegert, P., Tremaine, S.: The evolution of long-period comets. Icarus 137, 84-121 (1999)